Supplementary Materials For

GalNAc-T isozyme surface charge governs charge substrate preferences to modulate mucin type O-glycosylation

Collin Ballard[2], Miya Paserba[2], Earnest James Paul Daniel[2,3], Ramon Hurtado-Guerrero[4,5,6,7], Thomas A Gerken[2,1]

[2]Department of Biochemistry, Case Western Reserve University, Cleveland, OH 44106, USA, [3]present address Department of Pathology and Laboratory Medicine, Children's Hospital of Philadelphia, Philadelphia, Pennsylvania, USA, [4]BIFI and Laboratorio de Microscopías Avanzada (LMA), University of Zaragoza, Mariano Esquillor s/n, Campus Rio Ebro, Edificio I+D, Zaragoza, 50018, Spain, [5]Department of Cellular and Molecular Medicine, [6]Department of Dentistry, Faculty of Health Sciences, Copenhagen Center for Glycomics (CCG), University of Copenhagen, Copenhagen N DK-2200, Denmark, [7]Fundación ARAID, Zaragoza, 50018, Spain

[1]To whom correspondence should be addressed: Tel: 216-368-4556; Fax: 216-368-4223; e-mail: txg2@cwru.edu

Supplementary Figures:

Supplementary Tables

Supplementary Table SI: Sequences of peptides bound to GalNAc-Ts in the presence of Mn^{2+} and UDP

Supplementary Table SII: In vivo GalNAc-T N-glycosylation sites

Supplementary Table SIII: In vivo GalNAc-T O-glycosylation sites

Supplementary Table SIV: Previously unpublished enhancement values (EV) for hGalNAc-T11, PGANT35A (dT1) and hGalNAc-T6.

Supplementary Movies (as separate files)

Movies of the 250ns MD simulations for tgGalNAc-T3, hGalNAc-T12, and T2 bounds to charged peptides. Charged peptide residues are color coded blue for the positive Arg residues, red for the negative Asp residues, and white/green for the neutral Gly and Ala residues.

Supplementary Movie 1: 250nSec MD trajectory of the most active RR peptide bound to tgGalNAc-T3 (PDB 6S24)

Supplementary Movie 2: 250nSec MD trajectory of the least active DD peptide bound to tgGalNAc-T3 (PDB 6S24)

Supplementary Movie 3: 250nSec MD trajectory of the most active DR peptide bound to tgGalNAc-T12 (PDB 6XPU)

Supplementary Movie 4: 250nSec MD trajectory of the least active RD peptide bound to tgGalNAc-T12 (PDB 6XPU)

Supplementary Movie 5: 250nSec MD trajectory of the most active DD peptide bound to tgGalNAc-T2 (PDB5AJP)

Supplementary Movie 6: 250nSec MD trajectory of intermediately active GG peptide bound to tgGalNAc-T2 (PDB5AJP)

Supplementary Movie 7: 250nSec MD trajectory of least active RR peptide bound to tgGalNAc-T2 (PDB5AJP)

Supplementary Figure S1:

GalNAc-T template structures used for homology modeling of the GalNAc-Ts studied in this work (see Materials and Methods). A) Template structures, with the bound peptides used to model the GalNAc-Ts left-compact lectin structure (tgGalNAc-T3, PDB: 6S24), the extended lectin structure (hGalNAc-T2, PDB: 2FFU) and the right compact lectin structure (hGalNAc-T2 PDB: 5AJP). B) Sequences of the bound peptides in part A that were aligned onto each of our GalNAc-T homology structures. T* represents Thr-O-GalNAc.

Supplementary Figure S2:

Electrostatic surface potentials for all GalNAc-Ts studied. Each transferase was homology modeled against the three lectin domain orientations given in **Supplementary Figure S1** and are listed in the order given in **Figure 2**. The left column represents the lectin left compact structure (tgGalNAc-T3 PDB 6S24), middle column, extended lectin orientation (hGalNAc-T2 PDB: 2FFU), and right column, lectin right compact orientation (hGalNAc-T2 PDB: 5AJP). Bound peptides were aligned around the T/S-PXP sequence motif in each structure after superimposing the catalytic domains with bound peptides in PyMOL.

Supplementary Figure S3:

Electrostatic surface potentials for all GalNAc-Ts studied. Each transferase was homology modeled against the three lectin domain orientations given in **Supplementary Figure S1** and are listed in the order given in **Figure 3**. The left column represents the lectin left compact structure (tgGalNAc-T3 PDB 6S24), middle column, extended lectin orientation (human GalNAc-T2 PDB: 2FFU), and right column, lectin right compact orientation (human GalNAc-T2 PDB:

5AJP). Bound peptides were aligned around the T/S-PXP sequence motif in each structure after superimposing the catalytic domains with bound peptides in PyMOL.

Supplementary Figure S4:

Electrostatics of the LA repeat regions of the LDL receptor reveal defined regions of negative flanking charge. A) The electrostatic surface potential (blue) of GalNAc-T11. B) The location of the Thr residues of the low-density-lipoprotein receptor (LDLR) glycosylated by this isozyme. C) Electrostatic distributions of the LDLR surrounding these residues (black circles) showing areas of highly negative flanking charge (red) likely to enhance GalNAc-T11 binding (C).

Supplementary Figure S5:

Homology Models and electrostatic surface potentials of the PGANT based on the templates in **Supplementary Figure S1**. Left column *tg*GalNAc-T3 (PDB 6S24), second column *h*GalNAc-T2 (PDB: 2FFU), and third column *h*GalNAc-T2 (PDB: 5AJP) templates respectfully. The rightmost column gives the electrostatic surface potentials of the *h*GalNAc-T orthologues that were studied showing partial conservation of surface charge.

Supplementary Figure S6:

In-Vivo reported O-glycosylation sites and reported and predicted N-glycosylation sites for the studied GalNAc-Ts. Shown are the structures of *h*GalNAc-T1, -T3, -T4, -T5, -T6, -T7, -T11, -T12, -T13 & -T16 and *tg*GalNAc-T3 showing reported O-glycosylation sites (orange), reported (red) and/or predicted (blue) N-glycosylation sites, where the Thr or Asn residues are shown as spheres (see **Supplemental Table SII and SIII**). The shown bound peptide structures (green, blue and yellow), $^{2+}$Mn (purple) and UDP (green) were obtained from the homology model templates as described **Figure 2**. The N-terminal stem regions have been omitted in the

structures while the structures are shown to maximize visualizing the glycosites relative to the peptide binding site. Note the C-terminal Thr554 O-glycosite identified for GalNAc-T1 is absent in the PDB 6S24 template structure.

Supplementary Figure S7:

Comparison of the peptide substrate specificity of hGalNAc-T11 and its fly orthologue PGANT35A. A) Bar graph plot comparing hydrophobic residue enhancement values (EV) of hGalNAc-T11 (T11) and PGANT35A (T35A). B) Bar graph plot comparing hydrophilic residue enhancement values (EV) of hGalNAc-T11 (T11) and PGANT35A (T35A). C) Scatter plots of EVs for hGalNAc-T11 and PGANT35A showing their relative correlation. EV values are given in **Supplementary Table SIV**.

Supplementary Figure S8

Comparison of the peptide substrate specificity of subfamily Ic members hGalNAc-T3 and T6. A) Bar graph plot comparing hydrophobic residue enhancement values (EV) of hGalNAc-T3 (T3) and hGalNAc-T6 (T6). B) Bar graph plot comparing hydrophilic residue enhancement values (EV) of hGalNAc-T3 (T3) and hGalNAc-T6 (T6). C) Scatter plots of EVs for hGalNAc-T3 and T6 showing their relative correlation. EV values for hGalNAc-T6 are given in **Supplementary Table SIV**, EV values for hGalNAc-T3 have previously been reported (Gerken et al 2011).

Supplementary Figure S1:
Template Structures and peptides used for homology modeling of the GalNAc-Ts Studied

A) PDB Structure Templates from X-Ray Crystallography

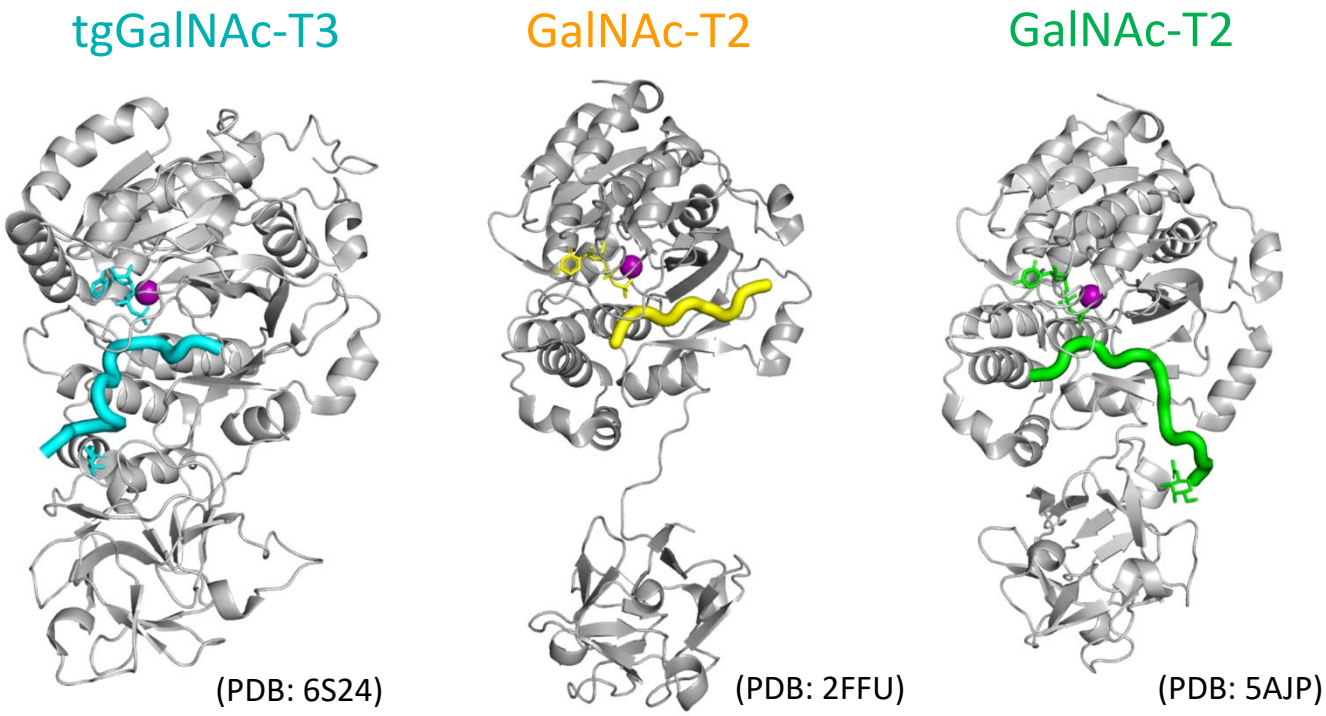

B) Bound Substrate Sequences

P3: GAT*GAGAGAGT<u>T</u>PGPG (PDB: 6S24)

EA2: PTTDST<u>T</u>PAPTTK (PDB: 2FFU)

AC13: GTTP<u>S</u>PVPTTSTT*SAP (PDB: 5AJP)

Supplementary Figure S2: Electrostatic Surface Potentials for the GalNAc-Ts in Figure 2

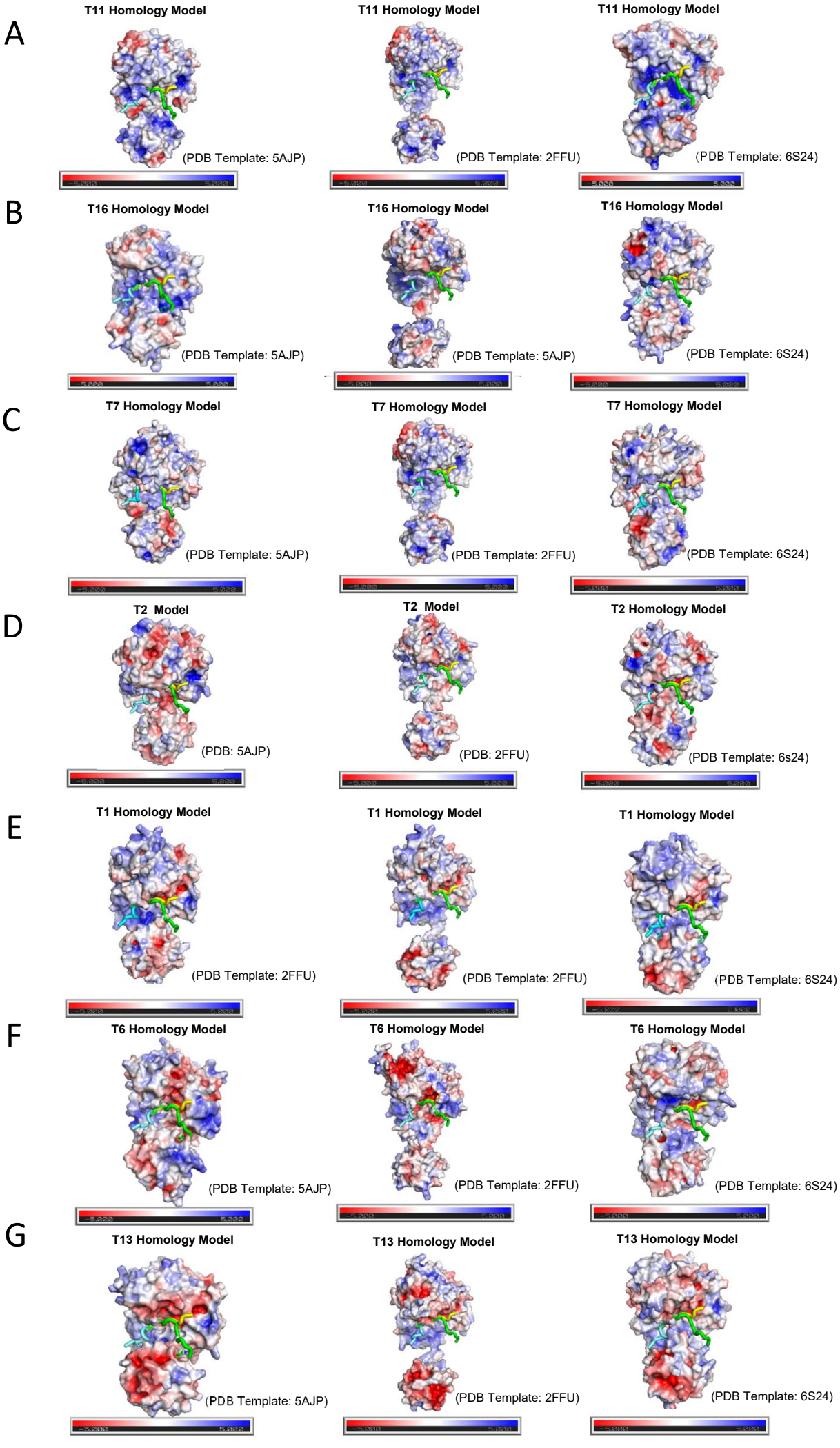

Supplementary Figure S2:
Electrostatic Surface Potentials for the GalNAc-Ts in Figure 3

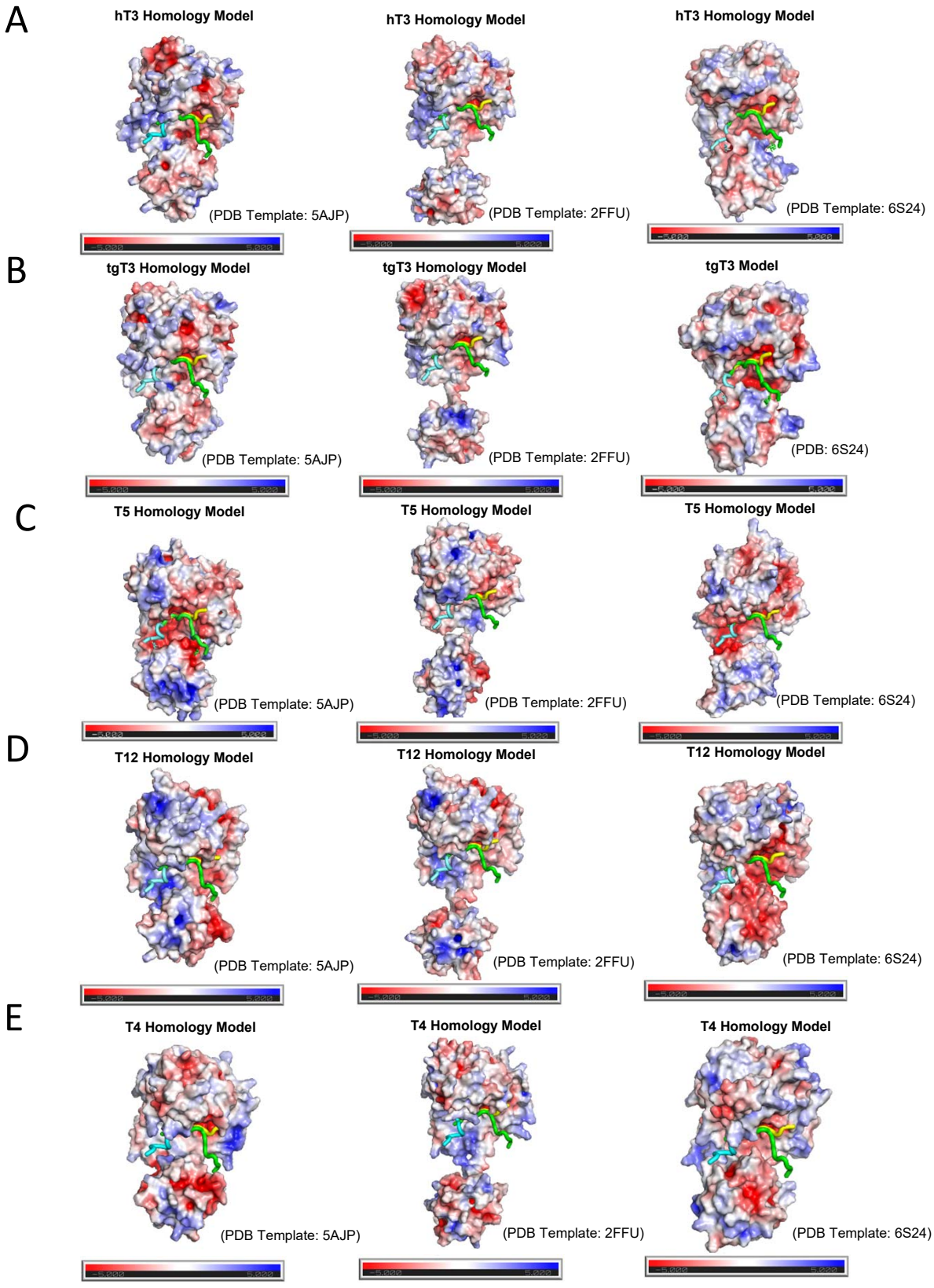

Supplementary Figure S4:
Electrostatics of the LA Repeat Regions of the LDL Receptor Reveal Defined Regions of Negative Flanking Charge

A

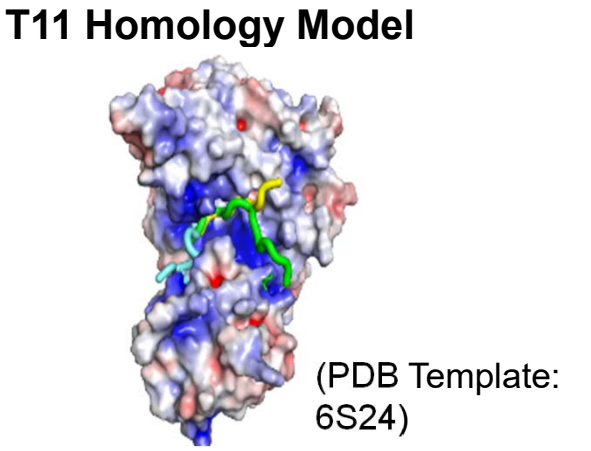

B

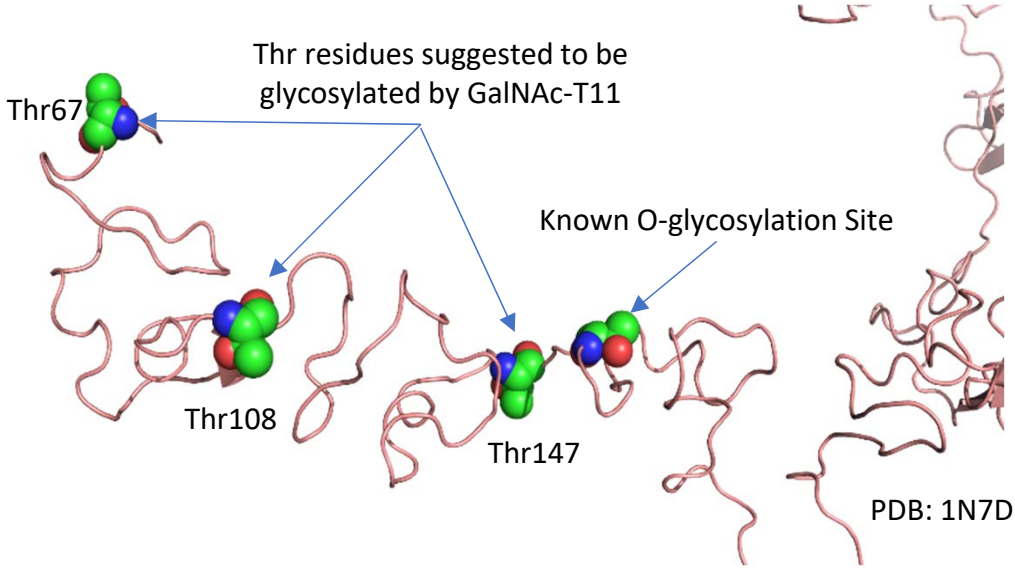

C

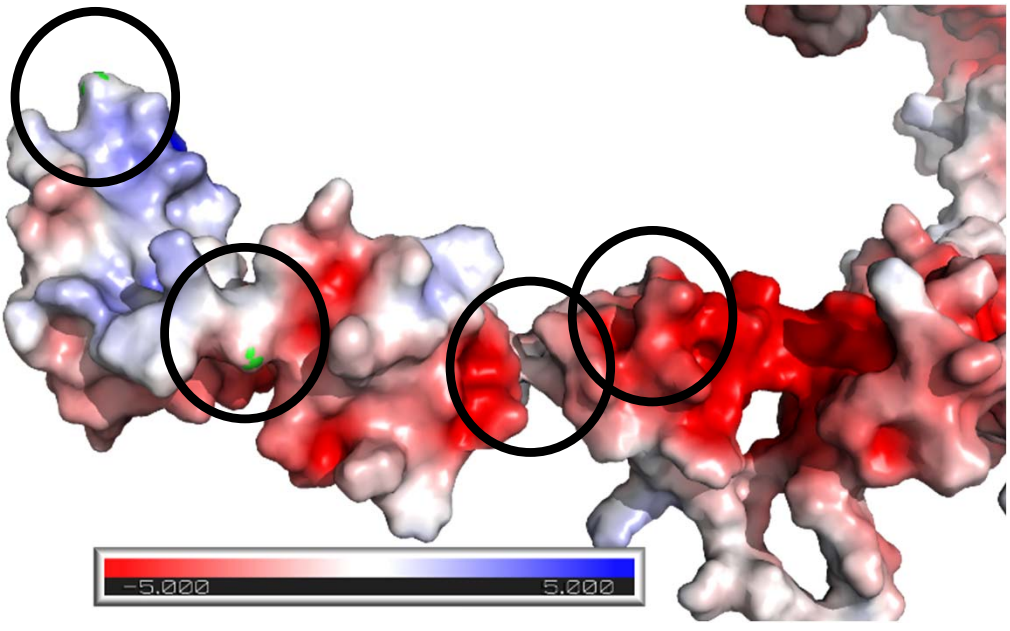

Supplementary Figure S5:
PGANT and Orthologue Surface Electrostatic Potentials

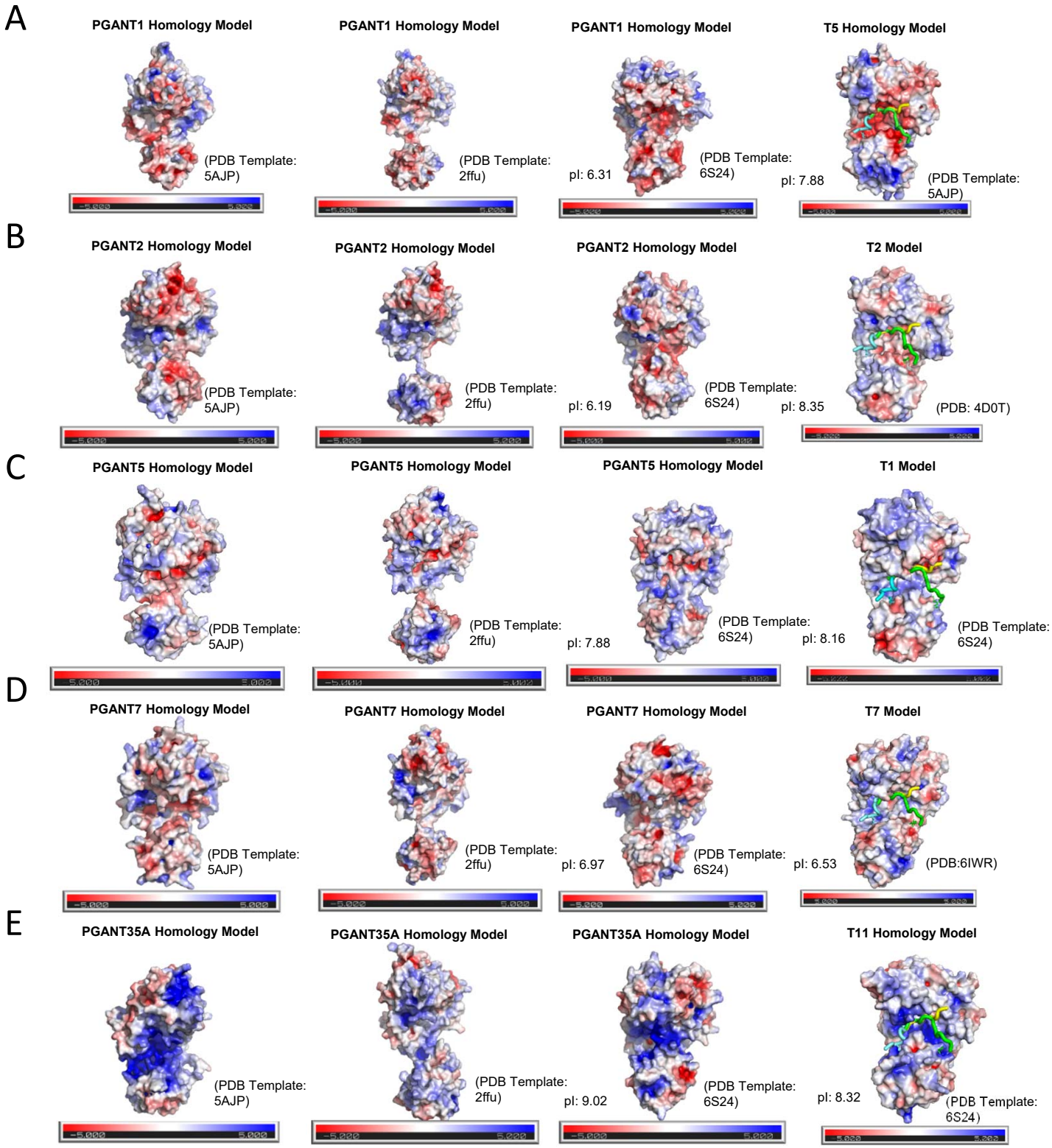

Supplementary Figure S6:
In-Vivo Reported O-Glycosylation and Reported and Predicted N-Glycosylation Sites on the Characterized GalNAc-Ts

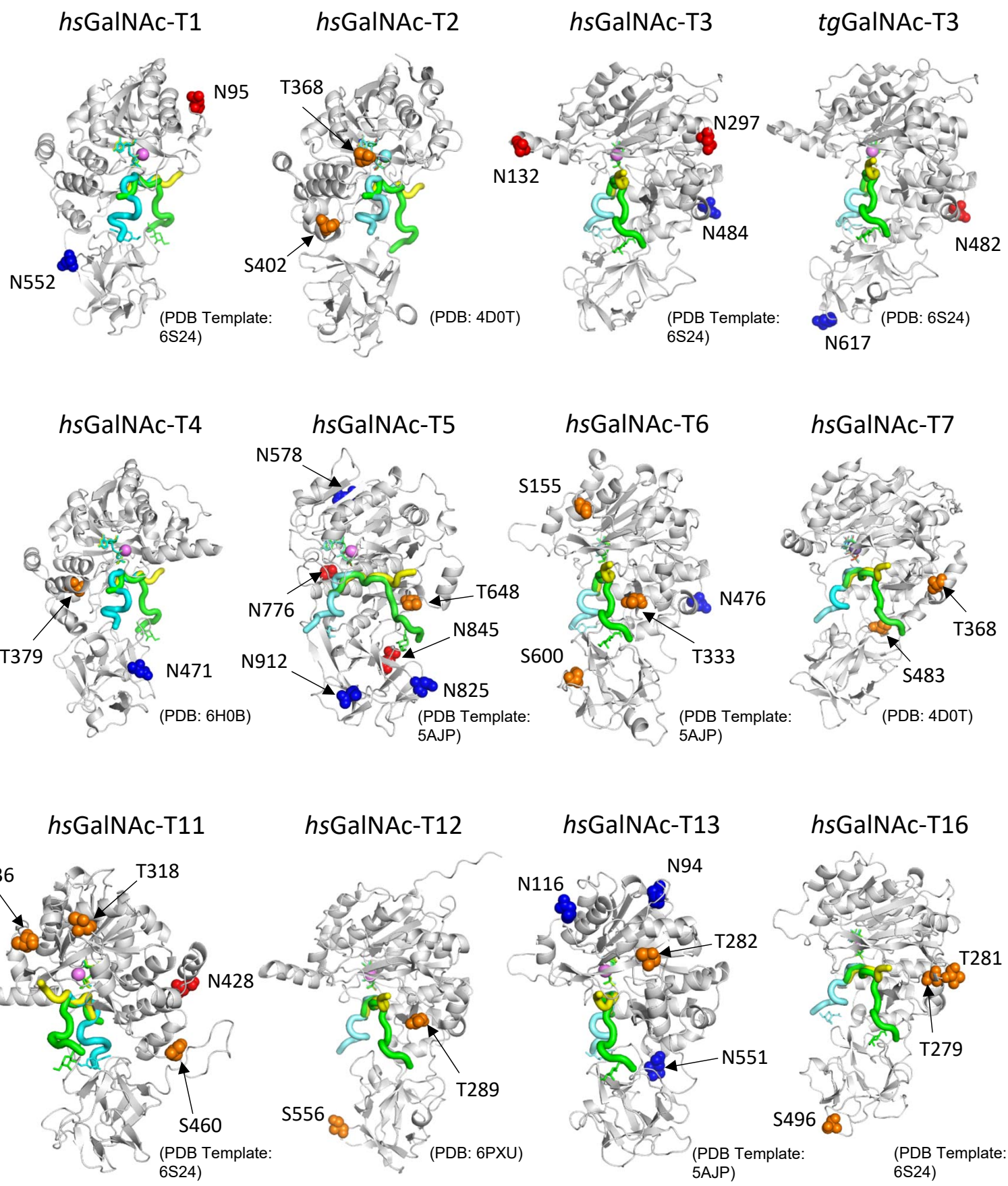

Supplementary Fig. S7: Comparison of GalNAc-T11 and PGANT35A Specificity

A

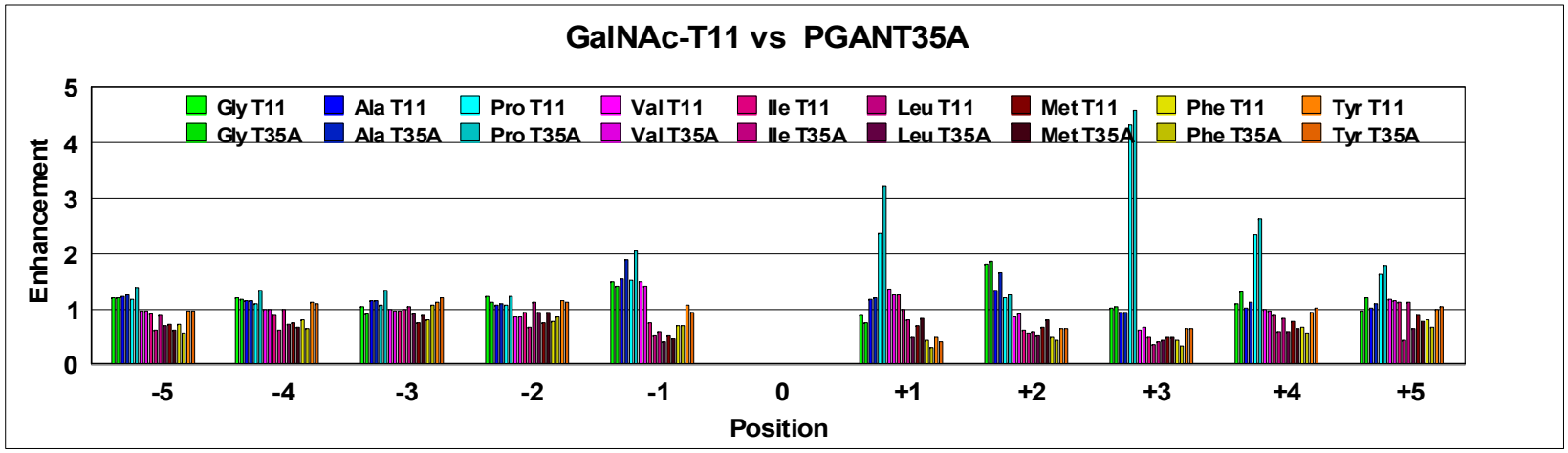

B

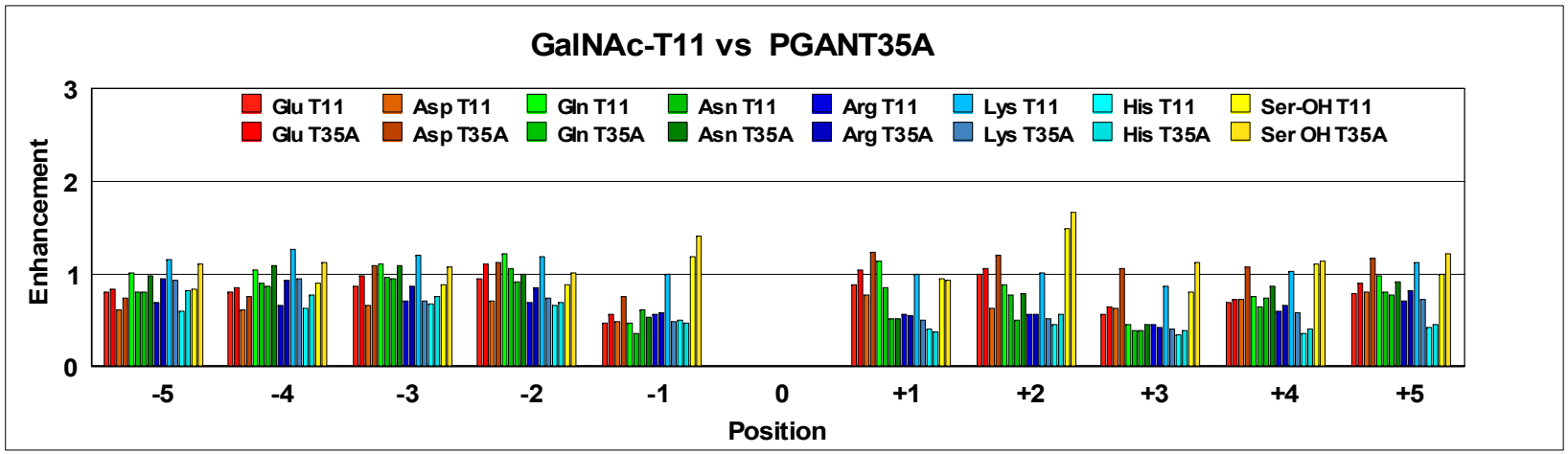

C

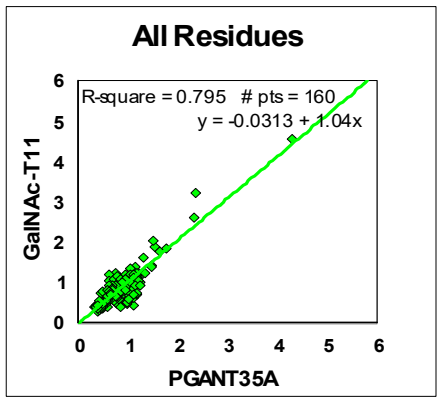

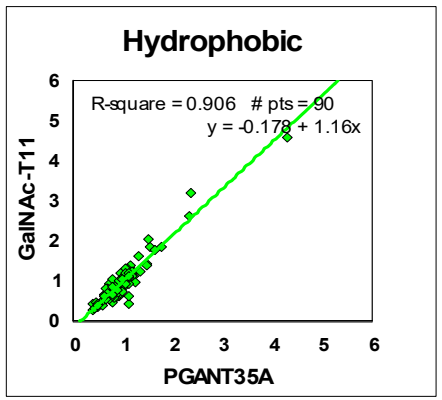

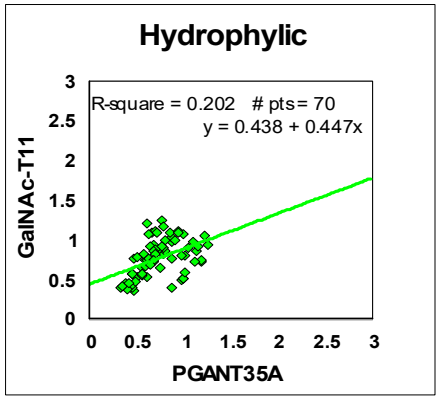

Figure S7

Supplementary Fig. S8: Comparison of GalNAc-T3 and GalNAc-T6 Specificity

A

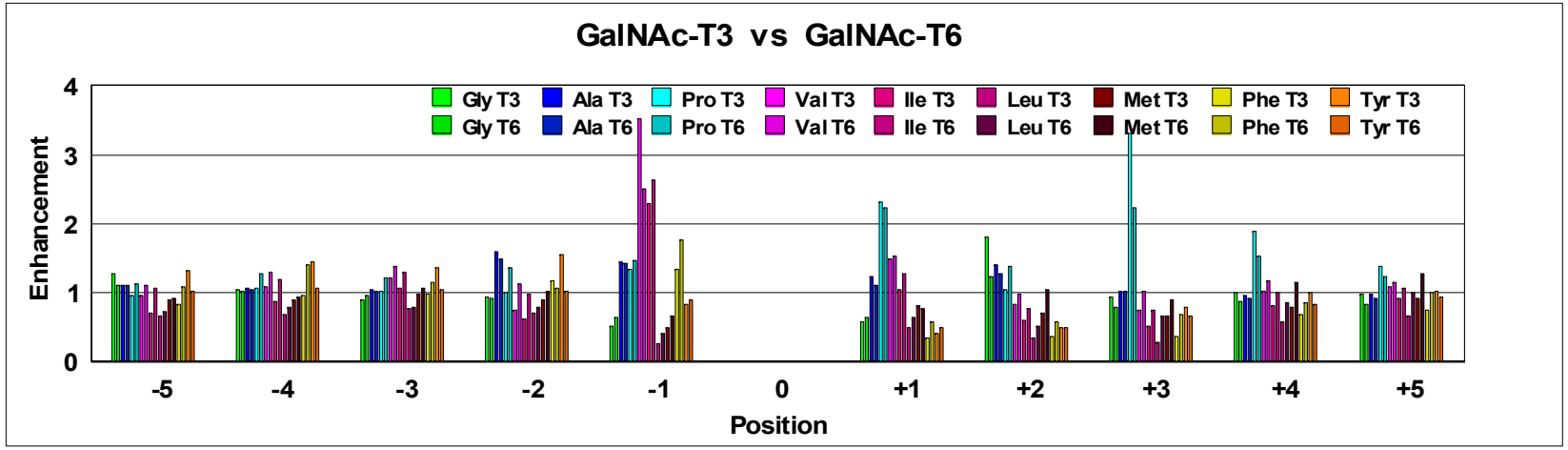

B

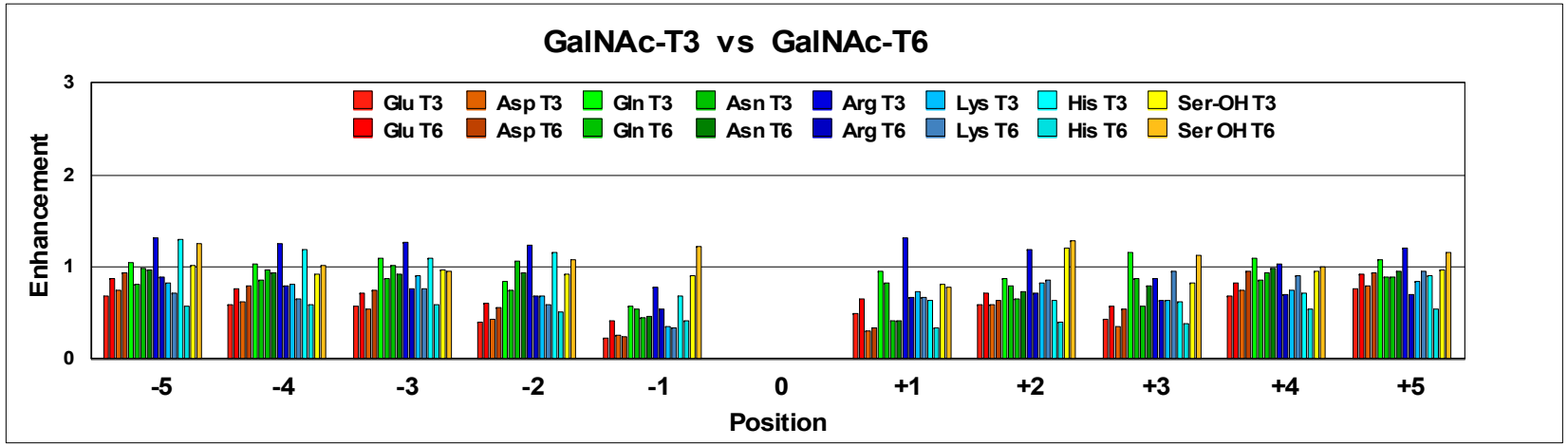

C

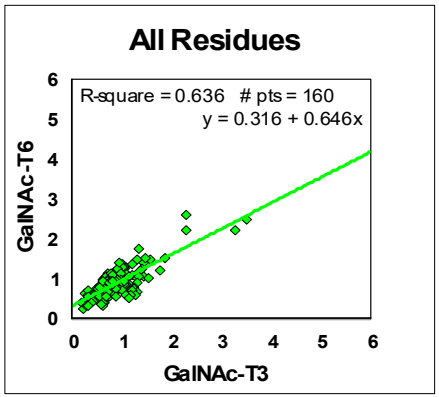

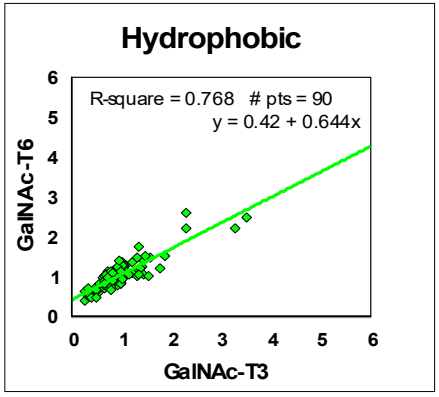

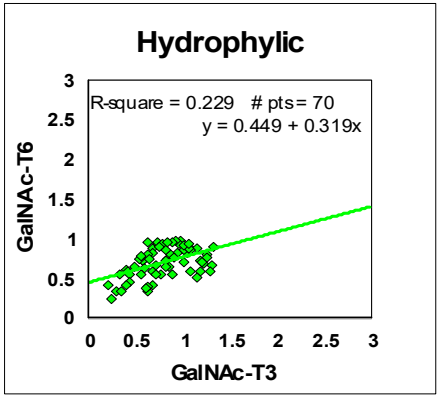

Figure S8

Supplementry Table SI

Peptide sequences of peptides bound to GalNAc-T crystal structures in the presence of Mn+2 and UDP shown in Fig 1.

GalNAc-T	PDB	Peptide	Sequence[a] .
T2	2FFU	EA2	ST**T**PAPTTK
T2	5AJP	AC13	TTP**S**PVPTTSTT*SAA
T2	4D0Z	mEA2	S**T**CPAA
T3	6S24	P3	AT*GAGAGAGT**T**PGP
T3	6S22	FGF23c	NT*PIPRRH**T**RSA
T4	6H0B	DGP6	GAT*GAGAGAGT**T**PGPG
T12	6PXU	DPG-5-17	GAGAT*GAGAGYYI**T**PRT*GAGA

[a]Acceptor site underlined and in bold, T* represents Thr-O-GalNAc.

Supplementry Table SII

In-Vivo reported and predicted N-glycosylation sites on the characterized GalNAc-Ts

Transferase	N-Linked Glycan Residue (Reported)	N-Linked Glycan Residue (Predicted)
*Hs*GalNAc-T1	N95[C]	N552[L]
*Hs*GalNAc-T2	None	None
*Hs*GalNAc-T3	N132[C], N297[C]	N484[C]
*Tg*GalNAc-T3	N482[C]	N617[L]
*Hs*GalNAc-T4	None	N471[L]
*Hs*GalNAc-T5	N776[C], N845[L]	N217[S], N256[S], N273[S], N316[S], N362[S], N395[S], N406[S], N578[C], N827[L], N912[L]
*Hs*GalNAc-T6	None	N86[S], N476[C]
*Hs*GalNAc-T7	None	None
*Hs*GalNAc-T11	N428[C]	None
*Hs*GalNAc-T12	None	None
*Hs*GalNAc-T13	None	N94[C/S], N116[C], N551[L]
*Hs*GalNAc-T16	None	None

[S] Residue located on N-terminal stem.

[C] Residue located on catalytic domain, in red.

[L] Residue located on the lectin domain, in red.

Supplementry Table SIII

In-Vivo reported O-glycosylation sites on the characterized GalNAc-Ts

Transferase	O-Linked Glycan Residue (Reported)
*Hs*GalNAc-T1	T554[L]
*Hs*GalNAc-T2	S5[S], S29[S], S59[S], S67[S], T70[S] S94[S], **T368[Cnp]**, **S402[Cnp]**
*Hs*GalNAc-T3	S124[S], T130[S], T131[S]
*Tg*GalNAc-T3	N.D
*Hs*GalNAc-T4	S46[S], S50[S], T56[S], S60[S], **T379[Cnp]**
*Hs*GalNAc-T5	S69[S], S70[S], T94[S], T108[S], T134[S], T138[S], T144[S], T149[S], S154[S], S155[S], S159[S], T163[S], T164[S], S172[S], S192[S], S200[S], S202[S], S204[S], S205[S], S207[S], S208[S], S221[S], T224[S], S231[S], S243[S], T244[S], S249[S], S262[S], T274[S], S275[S], T282[S], S292[S], T296[S], S300[S], S302[S], S320[S], T327[S], S356[S], S360[S], S367[S], S368[S], S369[S], S370[S], S379[S], T381[S], S402[S], S408[S], S418[S], T420[S], T429[S], S431[S], **T648[Ccp]**
*Hs*GalNAc-T6	T38[S], S48[S], S67[S], T81[S], S84[S], S88[S], T95[S], S123[S], S155[C], **T333[Ccp]**, S600[L]
*Hs*GalNAc-T7	T29[S], S36[S], S39[S], S103[S], T114[S], T119[S], T121[S], T368[C], **S483[Cp]**
*Hs*GalNAc-T11	S45[S], S51[S], T60[S], S64[S], S96[S], **T136[Ccp]**, T318[C], S460[CL]
*Hs*GalNAc-T12	T55[S], **T289[Ccp]**, S556[L]
*Hs*GalNAc-T13	S51[S], T282[C]
*Hs*GalNAc-T16	S34[S], S35[S], S47[S], T55[S], T61[S], T63[S], S65[S], S112[S], T279[C], T281[C], S496[L]

[S] Residue located on N-terminal stem.

[C] Residue located on catalytic domain, in red.

[Cp] Residue located on catalytic domain potentially affecting peptide substrate binding, in bold red.

[Cnp] Residue located on catalytic domain potentially affecting N-terminal substrate binding, in bold red.

[Ccp] Residue located on catalytic domain potentially affecting C-terminal substrate binding, in bold red.

[L] Residue located on the lectin domain, in red.

[CL] Residue located on the flexible linker connecting the catalytic and lectin domains, in red.

Notes for Supplementry Table SIV

Previously unpublished enhancement values (EV) for hGalNAc-T11, PGANT35A (dT1) and hGalNAc-T6.

EV values were obtained using 3 different random peptides, PVI, PVII and PVIII as described in the Materials and methods. EV values (and their standard deviations, SD) are given for -/+ 5 residues of the acceptor site at position 0. "n" represents the number of experimental determinations obtained for each amino acid residue, which range from 2 to 21 determinations depending on transferase.

Supplementary Table SIV:

Previously Unpublished Enhancement Values

hGalNAc-T11

n=5-21 unpublished		POSITION EV -5	EV -4	EV -3	EV -2	EV -1	EV 0	EV +1	EV +2	EV +3	EV +4	EV +5
G	Avg	1.20	1.18	0.92	1.13	1.42		0.75	1.86	1.04	1.30	1.20
	SD	0.20	0.17	0.25	0.21	0.29		0.32	0.31	0.29	0.24	0.21
A	Avg	1.25	1.14	1.15	1.09	1.88		1.21	1.64	0.93	1.12	1.10
	SD	0.14	0.10	0.16	0.13	0.35		0.23	0.43	0.23	0.11	0.15
P	Avg	1.39	1.33	1.34	1.22	2.06		3.22	1.26	4.58	2.62	1.79
	SD	0.31	0.26	0.29	0.28	0.63		0.88	0.18	1.14	0.59	0.25
V	Avg	0.96	0.99	0.96	0.87	1.40		1.26	0.91	0.67	0.96	1.14
	SD	0.06	0.07	0.16	0.10	0.23		0.18	0.11	0.14	0.11	0.15
I	Avg	0.62	0.62	0.99	0.68	0.51		1.00	0.57	0.35	0.60	0.44
	SD	0.11	0.08	0.53	0.12	0.10		0.21	0.19	0.07	0.05	0.37
L	Avg	0.70	0.74	0.92	0.94	0.41		0.49	0.51	0.45	0.61	0.64
	SD	0.11	0.10	0.23	0.24	0.13		0.07	0.12	0.30	0.10	0.40
M	Avg	0.63	0.67	0.88	0.93	0.45		0.84	0.82	0.49	0.65	0.78
	SD	0.05	0.06	0.21	0.25	0.08		0.20	0.28	0.15	0.05	0.06
F	Avg	0.57	0.64	1.07	0.87	0.70		0.29	0.44	0.32	0.57	0.68
	SD	0.14	0.11	0.53	0.40	0.26		0.09	0.18	0.07	0.10	0.14
Y	Avg	0.97	1.09	1.21	1.12	0.94		0.41	0.65	0.65	1.01	1.04
	SD	0.17	0.20	0.24	0.22	0.16		0.13	0.17	0.21	0.08	0.08
E	Avg	0.83	0.86	0.98	1.10	0.57		1.04	1.07	0.65	0.73	0.90
	SD	0.14	0.15	0.36	0.37	0.37		0.33	0.33	0.33	0.15	0.20
D	Avg	0.74	0.75	1.10	1.12	0.76		1.24	1.20	1.07	1.08	1.17
	SD	0.13	0.12	0.41	0.32	0.31		0.44	0.37	0.39	0.42	0.42
Q	Avg	0.80	0.89	0.97	1.06	0.36		0.86	0.77	0.40	0.65	0.81
	SD	0.19	0.22	0.20	0.20	0.13		0.18	0.15	0.06	0.09	0.18
N	Avg	0.99	1.09	1.09	1.00	0.54		0.52	0.79	0.45	0.88	0.92
	SD	0.17	0.16	0.17	0.16	0.13		0.13	0.13	0.05	0.07	0.06
R	Avg	0.95	0.93	0.87	0.85	0.58		0.54	0.57	0.43	0.67	0.82
	SD	0.44	0.36	0.34	0.27	0.21		0.18	0.15	0.16	0.12	0.13
K	Avg	0.93	0.94	0.72	0.74	0.49		0.51	0.52	0.41	0.59	0.72
	SD	0.27	0.30	0.35	0.27	0.30		0.28	0.26	0.25	0.30	0.29
H	Avg	0.82	0.77	0.75	0.70	0.47		0.37	0.57	0.39	0.41	0.46
	SD	0.28	0.20	0.15	0.13	0.13		0.13	0.13	0.10	0.09	0.09
S	Avg	1.19	1.19	1.22	1.15	1.50		1.27	1.81	1.30	1.24	1.32
	SD	0.13	0.10	0.13	0.13	0.11		0.36	0.28	0.19	0.11	0.14

Supplementary Table SIV continued:

PGANT35A (dT1)		POSITION										
n=2-6		**EV**	**EV**	**EV**	**EV**	**EV**	**EV**	**EV**	**EV**	**EV**	**EV**	**EV**
Ref: unpublished		**-5**	**-4**	**-3**	**-2**	**-1**	**0**	**+1**	**+2**	**+3**	**+4**	**+5**
G	Avg	1.20	1.19	1.06	1.22	1.50		0.88	1.80	1.03	1.10	0.98
	SD	0.16	0.11	0.15	0.10	0.22		0.15	0.26	0.11	0.10	0.12
A	Avg	1.24	1.15	1.16	1.06	1.54		1.17	1.33	0.94	1.02	1.02
	SD	0.12	0.08	0.10	0.06	0.24		0.05	0.10	0.03	0.04	0.04
P	Avg	1.17	1.11	1.07	1.07	1.51		2.36	1.20	4.32	2.33	1.64
	SD	0.33	0.25	0.19	0.20	0.29		0.48	0.11	1.18	0.50	0.27
V	Avg	0.96	1.00	1.00	0.85	1.48		1.37	0.85	0.63	1.00	1.18
	SD	0.06	0.11	0.11	0.08	0.40		0.16	0.09	0.05	0.19	0.19
I	Avg	0.92	0.88	0.96	0.93	0.75		1.26	0.62	0.50	0.88	1.12
	SD	0.01	0.00	0.02	0.01	0.02		0.14	0.01	0.02	0.05	0.02
L	Avg	0.90	1.00	1.04	1.12	0.60		0.79	0.59	0.42	0.83	1.13
	SD	0.04	0.01	0.02	0.01	0.08		0.04	0.08	0.09	0.08	0.08
M	Avg	0.72	0.75	0.76	0.75	0.51		0.69	0.66	0.48	0.77	0.89
	SD	0.01	0.01	0.00	0.00	0.01		0.03	0.01	0.02	0.02	0.04
F	Avg	0.74	0.82	0.80	0.79	0.69		0.43	0.50	0.44	0.67	0.81
	SD	0.01	0.01	0.01	0.00	0.02		0.01	0.02	0.03	0.04	0.01
Y	Avg	0.98	1.13	1.12	1.14	1.07		0.50	0.65	0.65	0.94	1.00
	SD	0.10	0.12	0.10	0.06	0.16		0.02	0.05	0.11	0.10	0.07
E	Avg	0.80	0.81	0.88	0.95	0.46		0.88	1.00	0.56	0.69	0.80
	SD	0.15	0.13	0.09	0.04	0.07		0.07	0.04	0.04	0.03	0.04
D	Avg	0.61	0.62	0.66	0.71	0.48		0.78	0.62	0.63	0.72	0.80
	SD	0.03	0.01	0.01	0.02	0.04		0.02	0.01	0.05	0.01	0.03
Q	Avg	1.02	1.05	1.11	1.23	0.48		1.14	0.88	0.46	0.75	0.98
	SD	0.12	0.09	0.07	0.04	0.00		0.05	0.00	0.01	0.01	0.04
N	Avg	0.81	0.87	0.96	0.92	0.61		0.52	0.51	0.38	0.75	0.77
	SD	0.06	0.07	0.04	0.09	0.01		0.01	0.03	0.03	0.02	0.02
R	Avg	0.69	0.66	0.71	0.70	0.57		0.56	0.57	0.46	0.59	0.71
	SD	0.15	0.14	0.14	0.15	0.13		0.13	0.14	0.18	0.14	0.15
K	Avg	1.16	1.27	1.20	1.19	0.99		1.00	1.01	0.87	1.03	1.13
	SD	0.08	0.09	0.13	0.14	0.22		0.18	0.15	0.15	0.12	0.10
H	Avg	0.59	0.64	0.68	0.66	0.50		0.41	0.46	0.34	0.36	0.43
	SD	0.10	0.12	0.12	0.14	0.06		0.05	0.06	0.02	0.03	0.06
S	Avg	0.83	0.90	0.89	0.89	1.18		0.95	1.48	0.81	1.11	0.99
	SD	0.01	0.05	0.05	0.06	0.07		0.09	0.09	0.05	0.15	0.09

Supplementary Table SIV continued:

hGalNAc-T6

		POSITION										
n=2-11		**EV**	**EV**	**EV**	**EV**	**EV**	**EV**	**EV**	**EV**	**EV**	**EV**	**EV**
Ref: unpublished		**-5**	**-4**	**-3**	**-2**	**-1**	**0**	**+1**	**+2**	**+3**	**+4**	**+5**
G	Avg	1.12	1.03	0.96	0.93	0.65		0.65	1.23	0.80	0.87	0.83
	SD	0.08	0.07	0.05	0.12	0.11		0.17	0.16	0.20	0.19	0.19
A	Avg	1.11	1.04	1.03	1.50	1.42		1.10	1.28	1.03	0.92	0.91
	SD	0.13	0.07	0.12	0.23	0.15		0.08	0.08	0.15	0.15	0.12
P	Avg	1.12	1.27	1.22	1.37	1.48		2.23	1.38	2.22	1.53	1.23
	SD	0.10	0.15	0.09	0.09	0.32		0.53	0.15	0.35	0.17	0.21
V	Avg	1.12	1.30	1.38	1.13	2.50		1.53	0.98	1.03	1.17	1.15
	SD	0.11	0.12	0.17	0.19	0.21		0.21	0.10	0.11	0.11	0.09
I	Avg	1.07	1.19	1.30	0.99	2.63		1.28	0.77	0.76	1.01	1.07
	SD	0.12	0.03	0.04	0.06	0.35		0.16	0.18	0.08	0.09	0.08
L	Avg	0.72	0.79	0.80	0.79	0.41		0.64	0.52	0.66	0.85	1.01
	SD	0.17	0.14	0.15	0.14	0.06		0.11	0.04	0.10	0.19	0.26
M	Avg	0.93	0.94	1.07	1.02	0.67		0.77	1.05	0.90	1.15	1.27
	SD	0.11	0.04	0.12	0.14	0.17		0.16	0.19	0.19	0.30	0.36
F	Avg	1.09	1.40	1.15	1.07	1.76		0.58	0.58	0.70	0.85	1.00
	SD	0.06	0.31	0.09	0.04	0.16		0.04	0.05	0.03	0.04	0.03
Y	Avg	1.04	1.07	1.05	1.02	0.89		0.49	0.49	0.66	0.84	0.93
	SD	0.14	0.14	0.12	0.11	0.04		0.05	0.09	0.12	0.08	0.11
E	Avg	0.88	0.77	0.72	0.61	0.42		0.65	0.72	0.58	0.83	0.93
	SD	0.19	0.14	0.11	0.14	0.12		0.14	0.11	0.11	0.14	0.16
D	Avg	0.94	0.80	0.75	0.56	0.24		0.34	0.63	0.55	0.95	0.94
	SD	0.12	0.09	0.11	0.08	0.07		0.07	0.07	0.09	0.07	0.07
Q	Avg	0.81	0.85	0.87	0.75	0.54		0.83	0.80	0.88	0.85	0.89
	SD	0.19	0.17	0.17	0.05	0.09		0.07	0.06	0.23	0.19	0.12
N	Avg	0.97	0.94	0.93	0.93	0.46		0.42	0.74	0.79	0.99	0.96
	SD	0.07	0.08	0.05	0.08	0.02		0.04	0.06	0.05	0.08	0.04
R	Avg	0.89	0.80	0.77	0.68	0.54		0.68	0.72	0.64	0.70	0.70
	SD	0.51	0.45	0.38	0.27	0.18		0.19	0.14	0.16	0.16	0.14
K	Avg	0.72	0.66	0.77	0.59	0.34		0.66	0.86	0.95	0.91	0.96
	SD	0.05	0.06	0.04	0.05	0.09		0.09	0.14	0.14	0.14	0.21
H	Avg	0.58	0.58	0.60	0.52	0.42		0.33	0.40	0.38	0.55	0.54
	SD	0.11	0.10	0.10	0.12	0.09		0.08	0.05	0.05	0.10	0.07
S	Avg	1.25	1.03	0.96	1.08	1.22		0.78	1.28	1.13	1.01	1.16
	SD	0.23	0.02	0.18	0.09	0.21		0.09	0.06	0.10	0.05	0.19